ResearchGate

See discussions, stats, and author profiles for this publication at: https://www.researchgate.net/publication/6757387

Conductance Maps by Electrochemical Tunneling Spectroscopy To Fingerprint the Electrode Electronic Structure

ARTICLE *in* ANALYTICAL CHEMISTRY · NOVEMBER 2006

Impact Factor: 5.64 · DOI: 10.1021/ac0603330 · Source: PubMed

CITATIONS
17

READS
19

4 AUTHORS, INCLUDING:

Ismael Diez-Perez
University of Barcelona
70 PUBLICATIONS **1,554** CITATIONS
SEE PROFILE

Fausto Sanz
University of Barcelona
190 PUBLICATIONS **2,954** CITATIONS
SEE PROFILE

Pau Gorostiza
IBEC Institute for Bioengineering of Catalonia
112 PUBLICATIONS **2,710** CITATIONS
SEE PROFILE

Available from: Pau Gorostiza
Retrieved on: 30 January 2016

Anal. Chem. **2006,** *78,* 7325−7329

Technical Notes

Conductance Maps by Electrochemical Tunneling Spectroscopy To Fingerprint the Electrode Electronic Structure

Ismael Díez-Pérez,† Aleix G. Güell,† Fausto Sanz,*,† and Pau Gorostiza*,‡

Laboratory of Electrochemistry and Materials (LCTEM), Department of Physical Chemistry, University of Barcelona, Martí i Franquès 1, 08028 Barcelona, Spain, and Centre de Referència en Bioenginyeria de Catalunya, Parc Cientific de Barcelona, Josep Samitier 1, Barcelona 08028, Spain

We describe a methodology to perform reliable tunneling spectroscopy in electrochemical media. Sequential in situ tunneling spectra are recorded while the electrochemical potential of the electrode is scanned. Spectroscopic data are presented as conductance maps or conductograms that show the in situ electronic structure of an electrode surface while it undergoes an electrochemical reaction. The conductance map or conductogram represents the redox fingerprint of an electrode/liquid interface in a specific medium and can serve to predict its electrochemical behavior in a quantitative energy scale. The methodology is validated studying the reversible oxidation and passivity of an iron electrode in borate buffer, and we describe the main quantitative information that can be extracted concerning the semiconducting properties of the Fe passive film. This methodology is useful to study heterogeneous catalysis, electrochemical sensing and bioelectronic systems.

The use of (electro)chemical-based techniques has become an essential part of the study of fundamental processes in fields such as sensing,[1] catalysis,[2] passivation/corrosion,[3,4] crystal growth,[5] or electron transport through (bio)organic molecules.[6] Although in situ measurements are essential to study directly the chemical−physical properties of electrode/liquid interfaces and the processes occurring therein, they are technically challenging and few techniques are available. Since the first applications of scanning tunneling microscopy (STM) to solid/liquid interfaces,[7] a variety of studies can be found showing spatial resolution up to the atomic scale.[8,9] STM also allows the implementation of an electrochemical cell through a four-electrode configuration (EC-STM), which enables control of the redox processes occurring at the electrode surface.[8] Electrochemical scanning tunneling spectroscopy (ECTS) provides a unique opportunity to probe in situ the local electronic properties of the electrode/liquid interface. Tao was the first to obtain spectroscopic information of a redox biomolecular system by using ECSTM imaging at different substrate potentials. [10a] In parallel, several papers demonstrated the practical realization of ECTS.[10b−14] However, several technical difficulties have hindered its wide application. To use ECTS as a robust electrochemical tool, it is essential to have the following: (i) accurate independent control of both tip and sample potential that ensures the chemical stability of the surfaces electrode, (ii) real reference electrodes that maintain the electrochemical potentials throughout the experiment, and (iii) suitable STM probes that provide a wide potential range and a low leak current during the fast tip voltage ramps used to minimize thermal drift. We have recently developed an electrochemical STM setup and tip preparation method to strictly satisfy all of these requirements.

An interesting system to assess with ECTS is iron electrode passivation, which is an extensively studied process[15−17] owing to its wide technological application and the economical impact that corrosion has on Fe and Fe-based alloys. Although the detailed

* Corresponding authors. E-mail: fsanz@ub.edu. phone: +34 4021240. Fax: +34 4021231. E-mail: pau.gorostiza@ub.edu. phone: +34 4037185. Fax: +34 4037181.

† University of Barcelona.

‡ Parc Cientific de Barcelona.

(1) Park, N.; Hahn, J. H. *Anal. Chem.* **2005**, *77*, 7100−7100.
(2) Maroun, F.; Ozanam, F.; Magnussen, M.; Behm, R. J. *Science* **2001**, *293*, 1811−1814.
(3) Ryan, M. P.; Williams, D. E.; Chater, R. J.; B. M. Hutton, McPhail, D. S. *Nature* **2002**, *415*, 770−774.
(4) Punckt, C.; Bölscher, M.; Rotermund, H. H.; Mikhailov, A. S.; Organ, L.; Budiansky, N.; Scully, J. R.; Hudson, J. L. *Science* **2004**, *305*, 1133−1136.
(5) Macpherson, J. V.; Unwin, P. R.; Hillier, A. C.; Bard, A. J. *J. Am. Chem. Soc.* **1996**, *118*, 6445−6452.
(6) Xu, B. Q.; Li, X. L.; Xiao, X. Y.; Sakaguchi, H.; Tao, N. J. *Nano Lett.* **2005**, *5*, 1491−1495.
(7) Sonnenfeld, R.; Hansma, P. K.; *Science* **1986**, *232*, 211−213.
(8) (a) Liu, H.-Y.; Fan, F. R. F.; Lin, C. W.; Bard, A. J. *J. Am. Chem. Soc.* **1986**, *108*, 3838−3839. (b) Gao, X.; Weaver, M. J. *Phys. Rev. Lett.* **1994**, *73*, 846−849. (c) Dietterle, M.; Will, T.; Kolb, D. M. *Surf. Sci.* **1998**, *396*, 189−197.
(9) Yao, H.; Yau, S.-L.; Itaya, K. *Appl. Phys. Lett.* **1996**, *68*, 1473−1475.
(10) (a) Tao, N. J. *Phys. Rev. Lett.* **1996**, *73*, 846−849. (b) Hugelmann, P.; Schindler, W. *J. Phys. Chem. B* **2005**, *109*, 6262−6267.
(11) Tomita, E.; Matsuda, N.; Itaya, K. *J. Vac. Technol., A* **1990**, *8*, 534−538.
(12) Azumi, K.; Araki, K.; Seo, M. *J. Electroanal. Chem.* **1997**, *427*, 15−21.
(13) Abadal, G.; Pérez-Murano, F.; Barniol, N.; Borrisé, X.; Aymerich, X. *Ultramicroscopy* **1996**, *66*, 133−139.
(14) Halbritter, J.; Repphun, G.; Vinzelberg, S.; Staikov, G.; Lorenz, W. J. *Electrochim. Acta* **1995**, *40*, 1385−1394.
(15) Büchler, M.; Schmuki, P.; Böhni, H. *J. Electrochem. Soc.* **1998**, *145*, 609−614.
(16) Buchler, M.; Schmuki, P.; Bohni, H.; Stenberg, T.; Mäntylä, T. *J. Electrochem. Soc.* **1998**, *145*, 378−385.

10.1021/ac0603330 CCC: $33.50 © 2006 American Chemical Society
Published on Web 09/20/2006

mechanism is still a subject of debate, the phenomenon of passivity is based on the spontaneous formation of an oxide film, a few nanometers thick, that effectively protects metal from corrosion.[18] Passive films can be created in an electrochemical cell by the controlled application of oxidizing electrochemical potentials in neutral and alkaline media. In the case of iron, the electronic properties of the surface can be driven from metallic (negative potential) to semiconducting Fe(III) oxide (positive potential), which offers a great variation to be tested by ECTS. The resulting semiconducting passive film has a large band gap, n-type properties, and a high doping density.[15−17,19] The electrochemical implications of these electronic properties are not completely understood, and speculative models have been proposed.[20,21]

In this contribution, we present a novel in situ analytical tool for the characterization of electrode/liquid interfaces based on ECTS technique. Our method allows us to measure conductance spectra of an electrode in the absolute energy scale and as a function of its oxidation state. These spectra can be directly compared to spectra acquired in air and vacuum, but are not affected by artifacts like the tip-induced band bending (see Supporting Information). Spectroscopic data are presented as 3-D conductance maps that outline the electronic structure of the electrode surface in the solution of interest. We have validated this methodology with an iron electrode that is reversibly oxidized in borate buffer solution throughout the entire electrochemical range.[17] The resulting conductance map of iron in borate, measured directly and locally at the nanoscale, is then useful to understand the macroscopic electrochemical behavior of iron.

EXPERIMENTAL SECTION

Chemicals. The recording liquid electrolyte (borate buffer solutions) was made of 0.3 M H_3BO_3 and 0.0375 M $Na_2B_4O_7 \cdot 10H_2O$ and gives a pH value of 7.5. Solutions were prepared with pro analysi purity grade chemicals from Merck (Darmstadt, Germany) and Milli-Q water of 18 MΩ·cm. All experiments were performed under an oxygen free atmosphere. This stage is very important since electroactive oxygen can be one of the main sources of the electrochemical current noise at the STM tip.[10] For that reason, in addition to 20-min nitrogen bubbling of all borate buffer solutions, the experiments were conducted in a sealed chamber under nitrogen atmosphere which was part of our STM system.

Substrate Preparation. The samples used in this study were mechanically polished polycrystalline iron disks 99.99%, 0.3 mm thick and 10 mm in diameter. The chemical purity of this surface was previously checked ex situ by X-ray photoelectron spectroscopy.[17] The polishing procedure involved a first step of grinding by silicon carbide polishing papers of 30-, 9-, 5-, 3-, and 1-μm particle size, successively, and then finishing with 0.3-μm aluminum oxide powder. Between each polishing step, the iron surfaces were sonicated in Milli-Q water and ethanol. Before each experiment, the samples were thoroughly rinsed in different solvents in order to remove organic contamination from the surface, followed by a final rinse in Milli-Q water. With this treatment, we obtained a mirrorlike surface with a mean roughness of typically less than 2 nm.

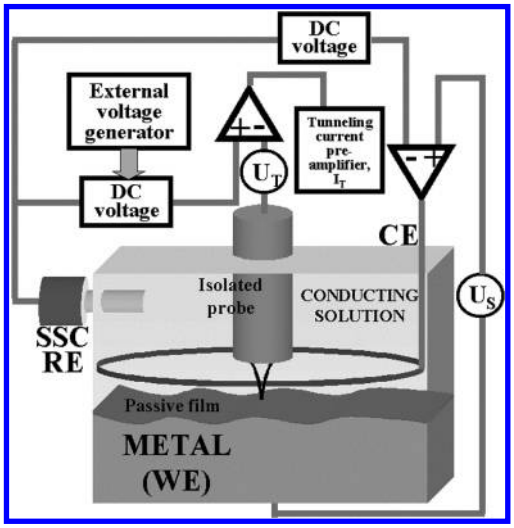

Figure 1. Simplified experimental setup showing the electrochemical cell with a 4-electrode configuration: metallic working electrode (WE), Pt counter electrode (CE), SSC reference electrode (RE), and STM tip electrode. This configuration allows independent voltage control of the electrochemical potentials U_T and U_S. STM bias is defined as U_S-U_T.

ECTS and Electrochemical Measurements. We used an electrochemical STM setup composed of a pico-SPM microscope (Molecular Imaging, Phoenix, AZ) controlled through a Nanoscope IIIa electronics (Veeco Instruments, Santa Barbara, CA), which was plugged to a signal access module that allows external application of fast voltage ramps using a signal generator (Agilent Technologies) and fast output data capturing in real time using a digital oscilloscope (Tektronix). This configuration allows stable and independent electrochemical potential control of both sample and tip (U_S and U_T, respectively), which were placed in a small electrochemical cell connected to a bipotentiostat (Picostat, Molecular Imaging), and a real miniaturized home-built Ag/AgCl reference electrode (SSC). A circular Pt wire served as a counter electrode. It is advantageous to quote directly U_T and U_S in the electrochemical scale (mV/SSC) instead of the sample bias ($U_S - U_T$), so that the Fermi level of tip and sample can be directly placed in energy diagrams. A scheme of our experimental setup is provided in Figure 1. Typically, our tunneling current versus U_T ramps spanned up to 2.5 V, covering the entire energy range of interest. Scan rates were up to 20 V/s and lasted less than 100 ms to minimize tip drift. These ramps require extremely well insulated STM tips in order to minimize electrochemical currents (faradaic and capacitive currents) exchanged at the tip and generated when U_T is rapidly ramped in a conductive media. Leak currents below 0.5 nA can be routinely obtained with proper tip preparation[22] and were further reduced by acquiring blank spectra at 3 nm of the surface at each U_S value.[13] Further technical information and other experimental details can be found in the Supporting Information. Cyclic voltammetry was performed with

(17) (a) Díez-Pérez, I.; Gorostiza, P.; Sanz, F. *J. Electrochem. Soc.* **2003**, *150*, B348−B354. (b) Díez-Pérez, I.; Gorostiza, P.; Sanz, F.; Müller, C. *J. Electrochem. Soc.* **2001**, *148*, B307−B313.
(18) Schönbein, C. *Ann. Phys. Chem.* **1836**, *37*, 390−399.
(19) Morrison, S. R., Ed. *Electrochemistry at Semiconductor and Oxidized Metal Electrodes*; Plenum Press: New York, 1980.
(20) Gerischer, H. *Corros. Sci.* **1989**, *29*, 191−195.
(21) Sato, N. *Corros. Sci.* **1990**, *31*, 1−19.
(22) Güell, A. G.; Díez-Pérez, I.; Gorostiza, P.; Sanz, F. *Anal. Chem.* **2004**, *76*, 5218−5222.

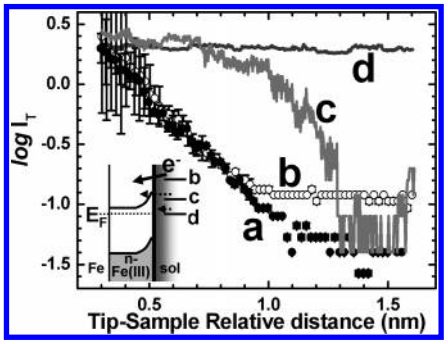

Figure 2. Averaged ($N \geq 5$) $I_T(s)$ plots at different U_T and Fe oxidation states (U_S). Exponentially decreasing currents correspond to stable tunneling conditions. Similar barriers are obtained at $U_T = -770$ mV, $U_S = -800$ mV (Fe(0), curve a) and $U_T = -770$ mV, $U_S = 500$ mV (Fe(III), curve b), which correspond to electron injection into the conduction band (see inset). On the iron(III) oxide surface, setting U_T within the band gap region gives rise to a nonexponential current behavior, as shown by example traces at $U_T = 100$ mV, $U_S = 500$ mV (curve c) and $U_T = 300$ mV, $U_S = 500$ mV (curve d).

Solartron electrochemical interface SI 1287 model using a standard electrochemical cell under static hydrodynamic conditions.

RESULTS AND DISCUSSION

Prior to the acquisition of current−voltage ECTS spectra, it was essential to evaluate the local energy barrier height (Φ) at every surface oxidation state in order to ensure the same initial tunneling conditions and to compensate the tunneling junction (see Supporting Information). Barriers Φ can be accurately calculated from the slope of the tip current (I_T) versus tip−sample distance (s), through the relation[14] $\Phi(\text{eV}) = 0.952\ (\text{d ln } I_T/\text{d}s)^2$. The I_T versus s plots of metallic and oxidized Fe electrode in borate buffer (Figure 2a and b, respectively) show a clearly exponential behavior. We have found that, using $U_T \leq -320$ mV, good tunneling conditions and reproducible barrier measurements are obtained for all U_S. At these U_T values, electrons are injected into the empty states of the metal or into the conduction band (CB) of the oxide (the CB edge of the Fe passive film is located at -320 ± 20 mV;[17] see inset plot of Figure 2). The obtained tunneling barriers are $\Phi = 0.30 \pm 0.06$ eV at $U_S = -800$ mV (corresponding to metallic Fe(0), Figure 2a) and $\Phi = 0.26 \pm 0.04$ eV at $U_S = +500$ mV (corresponding to passive Fe(III) oxide, Figure 2b). The fact that the same tunneling barrier is observed for the metallic and fully oxidized states indicates that, at these U_T, the rate-limiting step is electron tunneling through the liquid gap (Helmholtz layer[19]), with minor contributions due to the space charge region in the oxide. Using U_T near or within the band gap leads to poor tunneling conditions, as indicated by nonexponential behavior (Figure 2c) and a large scatter in the barrier measurements.[23] At these U_S, the tip is partially crashed on the surface as can be seen from the long retraction required to detach it (Figure 2d). It is thus essential to select U_T such that the same initial tunneling conditions are maintained throughout the entire conductance map (i.e., in all ECTS spectra at different U_S (oxidation state) values).

Once stable tunneling conditions are established, it is possible to obtain comparable tunneling spectra of the iron electrode

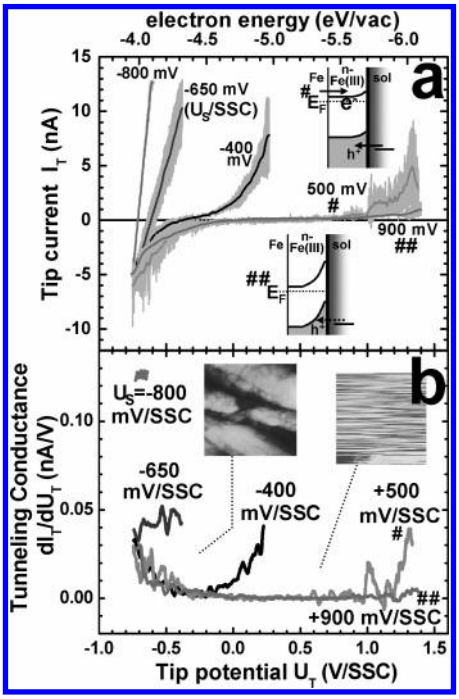

Figure 3. ECTS spectra of Fe in borate buffer at different oxidation states (U_S). Solid lines are averaged spectra, and gray bands indicate standard deviation ($N \geq 10$). (a) Spectra are linear for metallic Fe(0) ($U_S = -800$ and -650 mV) and show a double-exponential behavior as iron is oxidized to Fe(II) ($U_S = -400$ mV) and to Fe(III) ($U_S = 500$ and 900 mV). The positive branch is maintained by a current of electrons under slight electron depletion ($U_S = 500$ mV, upper inset, #) but is extinguished at stronger depletion conditions ($U_S = 900$ mV, lower inset, ##). (b) Tunneling conductance of ECTS spectra is calculated by differentiation of the curves in (a). Initial setpoint conditions were $I_T = 5$ nA and $U_T = -800$ mV. Electrochemical STM images of the Fe(III) surface ($U_S = 500$ mV, 400×400 nm^2) shows that imaging is only possible by electron injection into the conduction band ($U_T \leq -320$ mV).

surface as it is reversibly oxidized between $U_S = -1000$ and $+1100$ mV. At every U_S value, an initial $U_T \leq -320$ mV is set before disconnecting the STM feedback loop. ECTS spectra are then acquired by scanning U_T between -800 and $+1500$ mV while I_T is recorded. The $I_T(U_T)$ characteristics are shown in Figure 3a. $I_T(U_T)$ plots are differentiated to obtain the local conductance $\text{d}I_T/\text{d}U_T$ (Figure 3b), which is proportional to the density of states at the different electron energies.[14] Since they are measured versus a reference electrode in solution, tip current and conductance can be represented in an electron energy scale given in electronvolts versus the vacuum level[24] (top axis, Figure 3a). The same procedure is repeated at different U_S (electrode oxidation state), and series of ECTS are thus recorded.

ECTS spectra change strongly with the potential applied to the iron electrode U_S (Figure 3a), and these changes are directly related to the electrochemical state of iron within each potential range.[17] Between $U_S = -800$ and -650 mV, iron is fully reduced to metallic state (Fe(0)) and displays linear ECTS as corresponds to a high density of surface states or a high surface conductance (Figure 3a and b). At $U_S = -400$ mV, releasing of Fe^{2+}(aq) species into the solution gives rise to a hydrated Fe(II) oxide layer[16,17] with unknown electronic properties. Within this range and after

(23) Schreyer, A.; Eng, L.; Böhni, H. *J. Vac. Technol.* **1996**, *B14*, 1162−1166.

(24) Gerischer, H.; Ekardt, W. *Appl. Phys. Lett.* **1983**, *43*, 393−395.

film oxide growth, we find that ECTS spectra display a nonlinear characteristic with a region of low current flanked by two exponential branches (see Figure 3a and b). At $U_S = +500$ mV, a mostly Fe(III) oxide layer is formed whose n-type properties are well characterized.[16,17] In this region, ECTS spectra are nonlinear (one pound sign in Figure 3) and the separation between exponential branches is in good agreement with the reported band gap of the Fe passive film ($E_g = 1.6-1.9$ eV)[19] or LAMM phase (see Supporting Information).[25] At higher potentials $U_S \geq +800$ mV, the positive branch in ECTS decreases and almost disappears (two pound signs in Figure 3). The negative current branches in all spectra at negative U_T are due to electron injection from the tip into the CB of the oxide. The iron passive film can thus be imaged by electrochemical STM using $U_T \leq -320$mV[17] (Figure 3b, left inset), whereas no tunneling is possible within the band gap (Figure 3b, right inset). This further confirms the findings of Figure 2. The positive current branch of ECTS results from charge exchange with the valence band (VB), most likely by hole injection. Such a VB current could be maintained by recombination with electrons at slight depletion (upper inset in Figure 3a, one pound sign), but not under stronger depletion conditions at higher U_S (lower inset in Figure 3a, two pound signs). The reduction of the positive branch of the ECTS at $U_S = 900$ mV is then due to the large band bending in the semiconducting oxide and points out the low surface density of charge carriers under these conditions. Our results suggest that the energy barrier in the oxide, together with the absence of surface states in the band gap, limits the availability of reactants at the oxide surface and effectively passivates the electrode against further oxidation. Increasing the sample potential in the passive plateau results mostly in increasing the band bending inside the oxide and decreasing the electron concentration, without changing the band edge energy at the surface. This interpretation is in agreement with models proposed by Gerischer[20] and Sato[21] and demonstrates the capability of the method not only to obtain in situ the electronic structure of the electrode/electrolyte interface but also to see the availability of charge carriers at the electrode surface. Thus, ECTS provides direct information on the electronic structure of the electrode surface, and it is useful to elucidate the charge exchange mechanisms of the electrochemical processes occurring at the electrode.

To visualize ECTS data in a more compact form, conductance maps or conductograms (Figure 4a) are built from conductance curves (Figure 3b) acquired every 50 mV of U_S at a constant tunneling gap (see Supporting Information for more details). Conductance curves are stacked horizontally with U_T (i.e., electron energy) represented in the *y*-axis and the *x*-axis representing U_S (i.e., electrode oxidation state). Light and dark regions in the map correspond to high and low conductance, respectively, and hatched regions indicate saturation of our STM preamplifier but are not an intrinsic limitation of the technique. The full conductogram of the iron oxidation process in borate buffer solution at pH 7.5 is shown in Figure 4a. To ease the analysis, it is useful to align the conductogram with the corresponding voltammogram of the electrode in the same solution (Figure 4b).[17] As can be seen, the conductogram displays a horizontal bright stripe at high

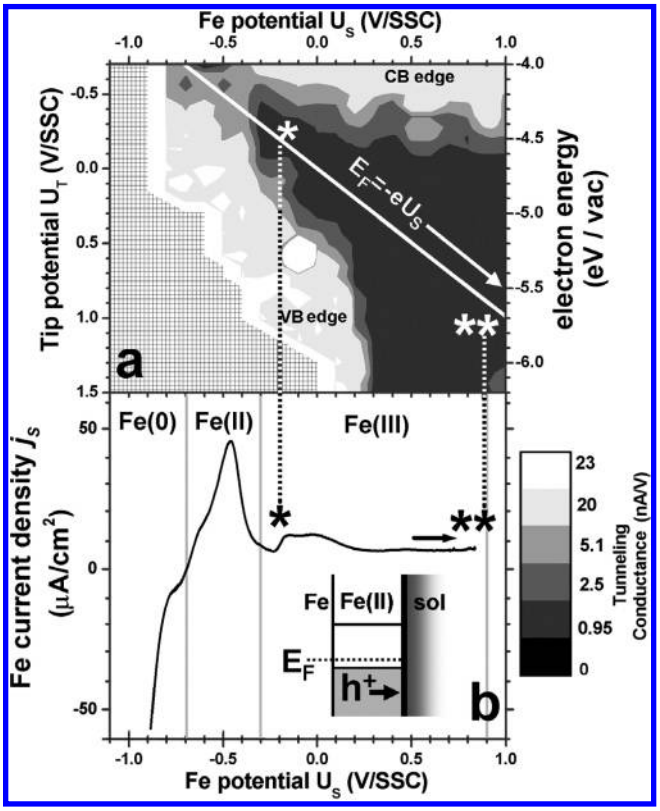

Figure 4. (a) Conductogram for the Fe oxidation process in borate buffer. ECTS spectra were obtained at constant tunneling gap (1.6 nm). The upper bright horizontal region corresponds to the conduction band edge at the surface and the lower bright region to the valence band edge. The diagonal line indicates the position of the Fermi level of the electrode. One asterisk (*) marks the onset of the Fe(II) → Fe(III) oxidation transition represented on the inset. Two asterisks (**) indicate the onset of transpassive breakdown of the electrode. (b) Cyclic voltammogram acquired on the same electrode showing the macroscopic oxidation process over the entire electrode surface (U_S scan rate of 5 mV/s).

energies (approximately constant with U_S) that corresponds to the CB edge at the surface. The VB edge is progressively shifted to lower energies (higher U_T values) as iron is further oxidized and it appears as a bright diagonal stripe. The dark region that separates CB and VB corresponds to the energy band gap as the electrode is being oxidized, and the line $E_F = -eU_S$ indicates the position of the Fermi level of the electrode. The position of the band edges and E_F allows us to build the experimental energy diagram of the electrode surface at every U_S, i.e., as a function of its oxidation state. Figure 4 allows us to compare at a glance the conductance map of the electrode obtained at the nanoscale with the voltammogram that characterizes its macroscopic electrochemical behavior. As can be seen, the onset of the Fe(II) → Fe(III) peak in the voltammogram[16,17] occurs when E_F approaches the VB region in the conductogram (indicated by one asterisk in Figure 4). High-conductance regions in the conductogram indicate that charge carriers can be exchanged with the electrode, thus reacting at the surface. In the case of the Fe(II) → Fe(III) peak, band bending under these conditions favors hole accumulation at the surface, which allows oxidation of the semiconducting electrode[19] (see energy diagram in the inset of Figure 4b). In the case of the passive plateau at higher potentials in the voltammogram, E_F does not approach any bright regions in the conducto-

(25) Toney, M. F.; Davenport, A. J.; Oblonsky, L. J.; Ryan, M. P.; Vitus, C. M. *Phys. Rev. Lett.* **1997**, *79*, 4282−4285.

gram and no reactions are observed. Note that the so-called transpassive breakdown[19,21] that occurs on the Fe electrode surface at $U_S \geq +1200$ mV can also be related to E_F approaching a high-conductance region (indicated by two asterisks in Figure 4). Conductograms thus provide a complete in situ view of the electronic structure of the electrode as it is being oxidized in a solution and allow us to understand the charge exchange mechanism of electrode reactions. The conductogram of an electrode constitutes the fingerprint of its electronic structure in a given electrolyte. As conductograms in different media become available, it will be possible to elucidate the mechanisms of complex electrochemical processes such as metal corrosion in aggressive media or charge exchange through modified electrodes.

CONCLUSIONS

In summary, we have developed a method to acquire reliable electrochemical tunneling spectra and we have validated it on a well-characterized electrochemical system: reversible iron oxidation in borate buffer at pH 7.5. ECTS was used for the first time to measure in situ the local tunneling barrier and tunneling spectra as a function of the oxidation state of the electrode. Spectroscopic data were presented as conductance maps or conductograms that show the in situ electronic structure of the electrode surface while it undergoes electrochemical reactions. Conductograms plot the free carrier density (electrons and holes) that constitutes the reactants on the surface electrode, as a function of electron energy and electrode potential (i.e., oxidation state). They help to understand the redox behavior of the electrode and can be used to predict ECSTM imaging conditions and charge exchange with redox probes in solution. In contrast to voltammograms, the acquisition of ECTS spectra is direct, local, and nondestructive, and their interpretation is not subjected to electric models of the interface as in the case of electrochemical impedance techniques.[15−17] Moreover, conductograms display an additional energy axis probed by the ECSTM tip (two-dimensional energy diagram) in front of the monodimensional spectroscopic data presented in previous ECSTM and ECTS works.[10−14] Given the local nature of ECTS measurements, conductance maps could be acquired over the surface of an electrode with nanometer spatial resolution, which is interesting to analyze the electrochemical heterogeneity at the nanoscale.[26] The spatial distribution of free charge carriers in an energy scale provided by ECTS would complement the measurements of electrochemical activity by scanning electrochemical microscopy.[27,28] The ECTS technique then has potential impact on the fields of corrosion, electrochemical sensing, heterogeneous catalysis, and bioelectronics and has been recently used to explain passivity breakdown on Fe electrodes as a function of pH,[29] in the presence of chloride,[30] and also to measure in situ energy barriers on thiol-modified Au(111) electrodes.[31]

(26) Burt, D. P.; Wilson, N. R.; Weaver, J. M. R.; Dobson, P. S.; Macpherson, J. V. *Nano Lett.* **2005**, *5*, 639−643.
(27) Amstrong, R. C. *Anal. Chem.* **1989**, *61*, 1099A−1104A.
(28) Serebrennikova, I.; Lee, S.; White, H. S. *Faraday Discuss.* **2002**, *121*, 199−210.
(29) Díez-Pérez, I.; Gorostiza, P.; Sanz, F. *Electrochim. Commun.* **2006**, *8*, 627−632.
(30) Díez-Pérez, I.; Vericat, C.; Gorostiza, P.; Sanz, F. *Electrochem. Commun.* **2006**, *8*, 1595−1602.
(31) Vericat, C.; Díez-Pérez, I.; Gorostiza, P.; Sanz, F. In 209th Meeting of The Electrochemical Society; Denver, CO, 2006.

ACKNOWLEDGMENT

This work was supported by a grant of MECD (Ministry of Education, Culture and Sports) under Project CTQ2004-08046-C02-01. P.G. acknowledges financial support of the MEC through the program Ramón y Cajal. We thank Miquel Salmeron and Francesc Pérez-Murano for comments on the manuscript and the Scientific-Technical Services of the University of Barcelona for use of their facilities.

SUPPORTING INFORMATION AVAILABLE

Additional experimental details of our electrochemical STM setup and the explanation of the methodological procedures (Figure S1). Supplementary electrochemical information on the electronic properties of the Fe passive film formed in borate buffer at pH 7.5 (Figure S2). This material is available free of charge via the Internet at http://pubs.acs.org.

Received for review February 22, 2006. Accepted June 22, 2006.

AC0603330